



## Experimental Investigation of The Optimal Location of PCM Capsules in a Hollow Brick Wall

Hayder M. Abbas <sup>a\*</sup>, Jalal M. Jalil  <sup>b</sup>, Sabah T. Ahmed  <sup>c</sup>

<sup>a</sup> Mech. Eng. Dept., University of Technology, Baghdad, Iraq. [20679@student.uotechnology.edu.iq](mailto:20679@student.uotechnology.edu.iq)

<sup>b</sup> Electromechanical Eng. Dept., University of Technology, Baghdad, Iraq.

<sup>c</sup> Mech. Eng. Dept., University of Technology, Baghdad, Iraq.

\* Corresponding author.

Submitted: 19/01/2021

Accepted: 23/02/2021

Published: 25/05/2021

### KEY WORDS

Phase Change Material (PCM), Thermal Insulation, Time Lag, and Decrement Factor.

### ABSTRACT

*In this paper, an experimental investigation of the integration of PCM capsules as insulation material into the outer or inner rows of hollow brick to find out the optimum location of the PCM capsules that give the best thermal performance of a wall. A test model consists of two identical cubical rooms was designed and fabricated to test the wall with and without PCM in a natural outdoor condition in Diwaniyah city in Iraq during the summer. The results show that the PCM will reduce the temperature of the inner side of the test wall and test room by 2.7 °C for the PCM capsules in the inner row while the reduction in both the inner surface temperature and the room due to the use of the capsules in the outer row was 1.9 °C. The time lag for the two cases was 1 hour. So that, the inner row location of PCM is the optimum location.*

**How to cite this article:** H. M. Abbas, J. M., Jalil, and S. T. Ahmed, "Experimental Investigation of The Optimal Location of PCM Capsules in a Hollow Brick Wall," Engineering and Technology Journal, Vol. 39, Part A, No. 05, pp. 846-858, 2021.

DOI: <https://doi.org/10.30684/etj.v39i5A.1980>

This is an open access article under the CC BY 4.0 license <http://creativecommons.org/licenses/by/4.0>

## 1. INTRODUCTION

Worldwide, the building sectors consumed a large amount of energy produced due to the utilization of cooling and heating systems to reach thermal comfort for people during hot summer and cold winter. In Iraq, about 38% of the total energy produced was consumed in the building sectors [1]. So that, to reduce the wasted power, it is necessary to increase the thermal performance of building envelopes by using insulation materials. The integration of phase-change materials in constructing walls is an effective method of improving the thermal performance of the walls due to their thermal properties. Besides its low thermal conductivity, PCM can absorb large quantities of heat during charging and release this heat during the process of discharging which reduces the cooling or heating load and translates the maximum load to a different time. Many studies investigated the utilization of PCM as an insulator in buildings walls are conducted. Alawadhi [2]

tested numerically a hollow brick filled with PCM at a different location. He found that the reduction in heat gain increases with the increase of PCM amount and the best location of the PCM cylinder is in the centerline of brick. Another outdoor test of several cubicles provided constructed from conventional and alveolar brick containing PCM and provided with heat pumps for cooling made by [3]. They found that the reduction in the peak temperature of the inner wall surface by 1°C, smooth the daily fluctuation of temperature and a reduction of 15% in the electrical power which led to a reduction in the CO<sub>2</sub> emission about 1–1.5 kg/year/m<sup>2</sup>. Quanying et al. [4] tested three different structures of the wall, include shape stabilized PCM wallboard composite of paraffin mixture and high-density polyethylene. They found that a small reduction in the surface temperature and heat flow. Also, the energy-saving effect of the shape-stabilized PCM walls prepared by the lamination interpolation method are better than that of the shape stabilized PCM walls by direct mixing. Kong et al. [5] conducted three tested rooms, two with a layer of PCM, one placed on the interior side of the wall (PCMIW) and the other placed at the exterior side of the wall (PCMOW), while the last room without PCM. For the inside surface temperature of the south wall, the reduction of the average temperature and peak temperature was 0.96 °C and 2.63 °C for PCMIW, respectively, while the reduction was 0.41 °C and 2.46°C for PCMOW, respectively. Jin et al. [6] conducted an indoor test of a dynamic simulator room provided by PCM layers integrated into the walls at different locations. The results revealed that the optimum location of the PCM layer is close to the interior side where the reduction of heat flux and time lag was 41% and 2 h, respectively. Also, Zwanzig et al. [7] tested a PCM layer integrated into the wall and ceiling at a different location. The results show that the optimal location of the PCM layer depends on the resistance value between the PCM layer and the exterior wall. The PCM reduces energy consumption in the summer. Lee et al. [8] used a plug and play wall which was easy to install and dismantled and provided with a PCM thin layer tested in a real condition. They found that the reduction of average daily heat flux was 27.4% and 10.5%, while the reduction in the peak heat flux was 67% and 80.2% in the south and west-facing wall. Also, the time lag was delayed from 2 to 3 hours. Guarino et al. [9] tested a PCM layer adjacent to the interior side of the wall of the hut that paced in a climatic chamber. Their results showed a reduction of about 20% of energy consumption. Hasan et al. [10] conducted three insulated chambers, one without PCM and two rooms with PCM (one provided by the PCM layer closest to the interior surface and the other PCM layer close to the exterior surface). They found that the PCM layer adjacent to the indoor show the best performance with a reduction of inside wall temperature, heat gain, and time lag were 8.5%, 2.6h, and 44% respectively. Jin et al. [11] examined numerically a thin layer of PCM integrated at different locations into walls. The optimal location of the PCM layer that gives a higher thermal performance was found close to the internal surface of the wall. Fateh et al. [12] presented numerically a PCM layer integrated at a different location within the wall. They found a reduction in energy saving up to about 75% of the heat load. Ning et al. [13] examined a PCM layer integrated into the building wall. The results found a significant reduction in the temperature fluctuation in the room, the PCM amount increase will decrease the fluctuation while the increase of PCM melting temperature reduces the temperature variation. Rafie et al. [14] conducted an indoor test of two walls, the first without PCM while the second provided with 20% volume percentage PCM mixed mortar at the external layer of the wall. A reduction in the internal surface temperature of the wall by 1.6 °C was recorded. Kumar et al. [15] examined a PCM integrated into hollow brick. The results demonstrated that the maximum reductions of room temperatures were 6°C and 2°C for January and July, respectively.

In this study, a system consists of two identical cubical rooms was designed and fabricated, the first room is a test room (PCM room) which provided a treated wall (wall with PCM capsules) and the second room is standard (room without PCM or room provided with a domestic wall). Two treated walls with PCM were tested in the test room due to the location of PCM and compared with the domestic wall to investigate the thermal performance of each wall and find out the optimal location of PCM.

## 2. MODEL DESCRIPTION

Firstly, the Test model was designed with SOLIDWORKS software, as shown in Figure 1, and then fabricated as shown in Figure 2. The PCM model consists essentially of two identical cubic rooms with an intermediate control chamber in between. The first room is a standard room and the

second room is a test room (PCM room), while the control room contains recording equipment such as a computer and other data loggers. The test room and standard room both had an ice container as a cooling system as illustrated in Figure 1. Except for the south wall, the other rooms' sides are manufactured from different layers of sandwich panels with a thermal conductivity "strong polyisocyanurate foam core with an external and internal plate in steel 5 cm thick" ( $0.034 \text{ W m}^{-1} \text{ K}^{-1}$ )[1]. Also, the foam was used to fill all the cavities in the model to stop the ventilation from or to the rooms. The two rooms are the same and each has internal dimensions ( $0.45 \text{ m length} \times 0.45 \text{ m width} \times 0.45 \text{ m height}$ ), the thickness is  $0.1 \text{ m}$  for both west and east walls,  $0.15 \text{ m}$  for the roof, and  $0.2 \text{ m}$  from the floor. The floor of the rooms was elevated from the ground with  $0.2 \text{ m}$  by Thurmaston brick, to minimize the thermal transmission from the ground to the interior of the rooms.

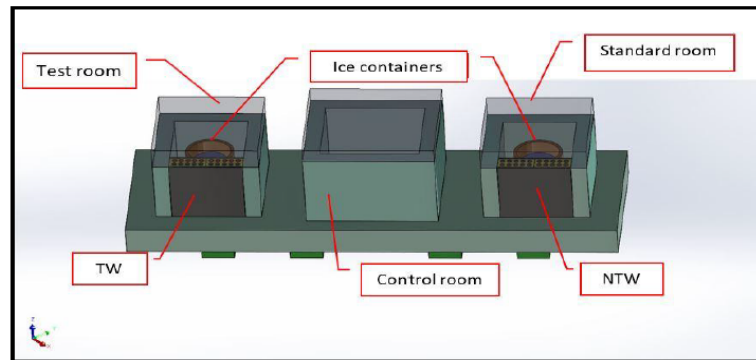


Figure 1: Schematic of Test Model

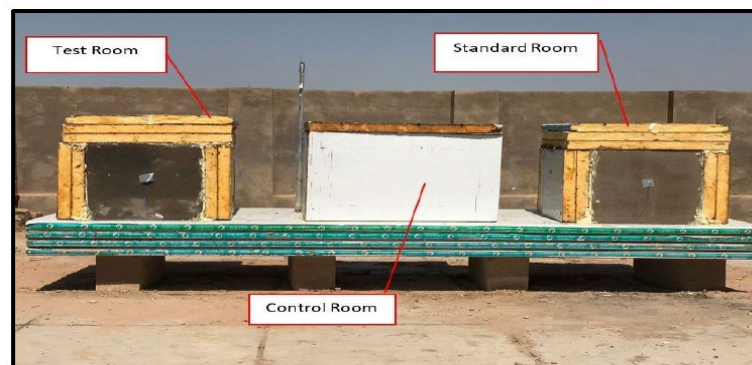


Figure 2: Test Model

### I. Cooling System

Because of the electric energy supplied in Iraq is lacking and intermittent, the ice is used to cool the system instead of the air conditioner. Both test rooms contain an ice container that is fixed in the center of each room, as illustrated in Figure 3. The two ice containers are identical and each isolated container on all sides except the top and contains  $9.35 \text{ kg}$  of ice. The ice plays an important role in the decrease of the temperature in rooms by natural convection to avoid global warming and keep the room temperature profile within an acceptable range of comforts.

### II. Standard Room

It is a room set up for comparison to test the south wall. The south wall in this room is an Iraqi domestic wall without PCM (NTW) consist of a  $1 \text{ cm}$  of the mortar layer with thermal conductivity of  $1.16 \text{ W m}^{-1} \text{ K}^{-1}$  [14] and a hollow bricklayer with a thickness of  $10.2 \text{ cm}$  with thermal conductivity of  $0.812 \text{ W m}^{-1} \text{ K}^{-1}$  [14] followed by  $1 \text{ cm}$  of mortar layer. The cavities of hollow bricks are filled with mortar as shown in Fig.3 and Figure 4.



Figure 3: Standard Room

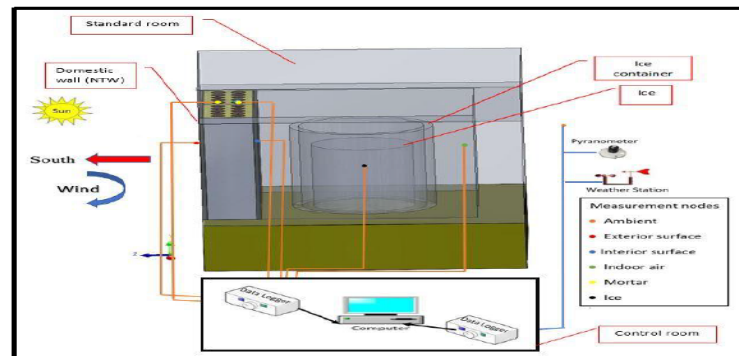


Figure 4: Schematic of Standard Room

### III. PCM Encapsulation

The PCM encapsulated into identical sealed small tubes (29 mm diameter  $\times$  70 mm height  $\times$  0.4 mm thickness) dimensions for each one as shown in Figure 5. The capsules are made from aluminum with thermal conductivity ( $221 \text{ W m}^{-1} \text{ K}^{-1}$ ) [12]. The amount of PCM inside one capsule is 35 grams occupied about 95% of the total volume of the capsule, while the total weight of the capsule is 55 grams. Sixty capsules are fabricated, all capsules are identical, and inserted into the cavities of the inner rows of hollow bricks close to the interior side of the test wall (PCM wall). All the capsules were tested for over  $90^\circ \text{C}$  to make sure that no leakage of PCM from the capsules. The Properties of PCM [14] showed in Table I.

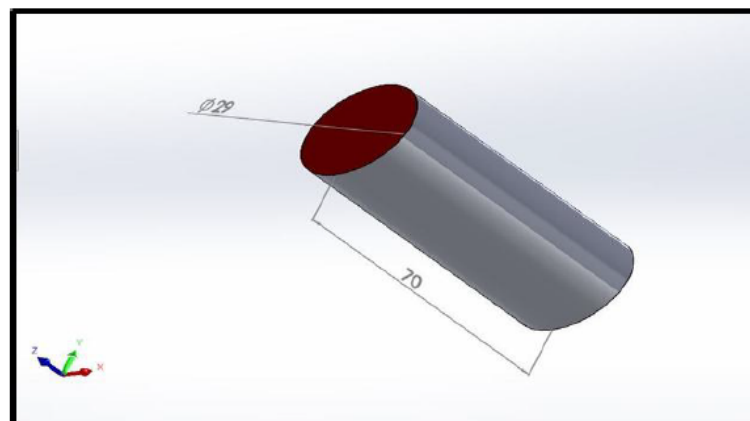


Figure 5: PCM Capsule

**TABLE I: Thermophysical properties of Paraffin wax [14]**

Property	Values
Melting temperature range	38-43 °C
Congeaing temperature range	43-37 °C
Heat storage capacity	174 kJ/kg
Specific heats in both solid and liquid states	2 kJ.kg <sup>-1</sup> . k <sup>-1</sup>
Density in solid state	880 kg/m <sup>-3</sup>
Density in liquid state	760 kg/m <sup>-3</sup>
Volume expansion (solid/liquid phase change)	16%
Thermal conductivity in both solid and liquid state	0.2 Wm <sup>-1</sup> . K <sup>-1</sup>

#### IV. Test Model-A

In this test, the test room in the model is modified by using PCM capsules as shown in Figure 6 the test room-A shown in Figure 7 and Figure 8. This room is identical to the standard room except the south wall treated with PCM (TW-A), where the PCM capsules inserted in the inner rows of hollow bricks close to the interior side of the wall instead of mortar that used in the NTW in a standard room.

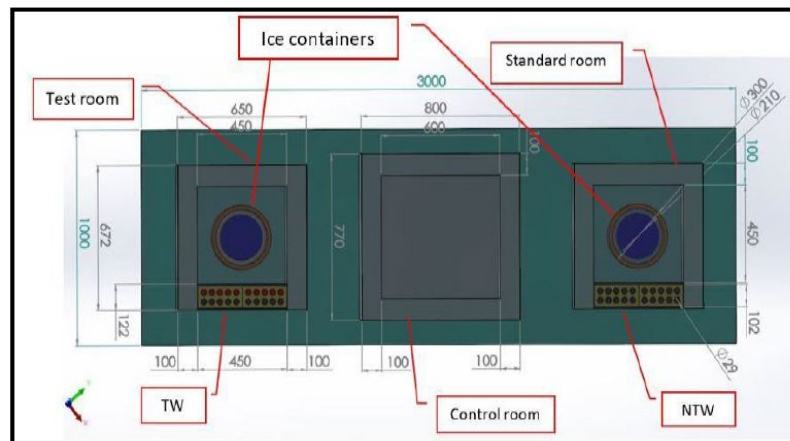


**Figure 6: Top View of Test Model-A**



**Figure 7: Test Room-A**

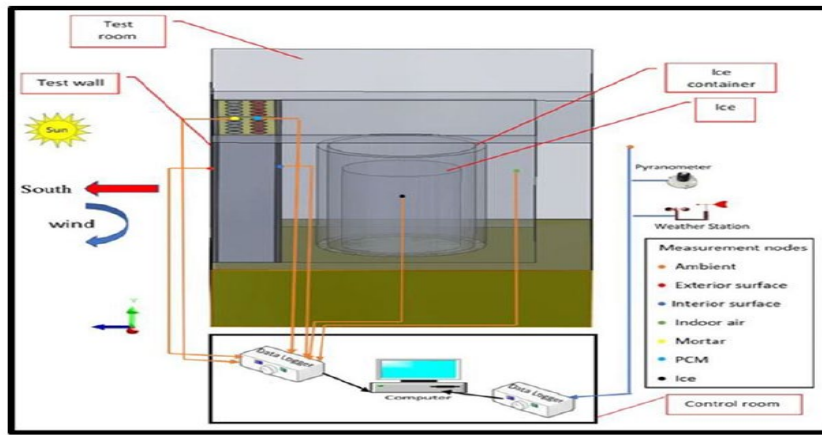


Figure 8: Schematic of Test Room-A

**V. Test Model-B**

In this test model, the test room model is modified by using PCM capsules as shown in Figure 9. The test room B is shown in Figure 10 and Figure 11. This room is identical to the standard room except the south wall treated with PCM (TW-B), where the PCM capsules inserted in the outer rows of hollow bricks close to the exterior side of the wall instead of mortar that used in the NTW in a standard room.

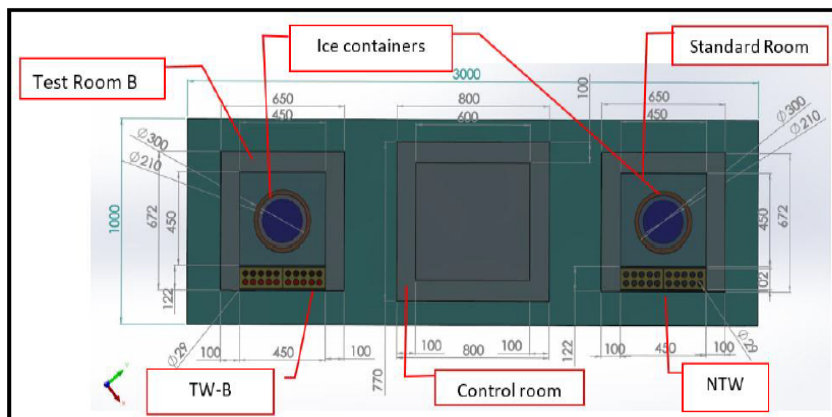


Figure 9: Top view of Test Model-B

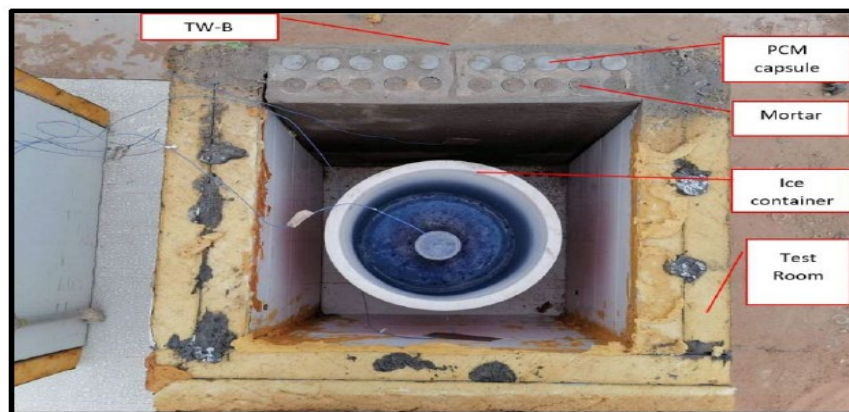


Figure 10: Test Room B

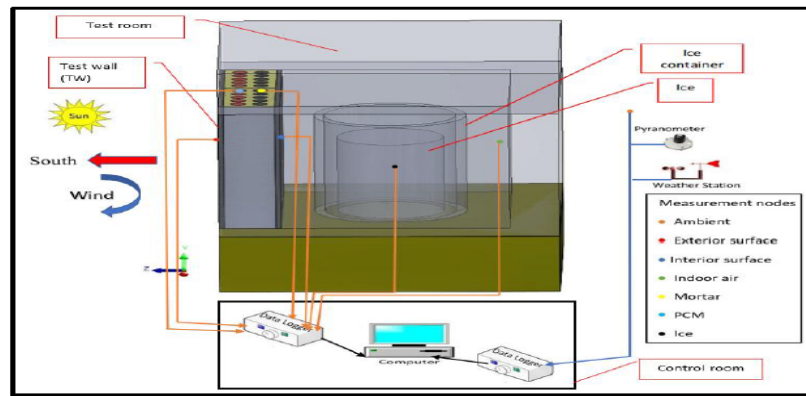


Figure 11: Schematic of Test Room B

### 3. MEASUREMENT INSTRUMENTS

#### I. Temperature Data Logger

Data acquisition from Applent company named AT4208 Multi-channel temperature meter with 8 sectors connected to K-type thermocouple probs. The thermocouple was calibrated with maximum errors  $\pm 0.2$  °C and then used to measure the temperature. The data logger was connected to a computer using special software to record the temperature every 15 minutes along 24 hours of the day. The sensors were fixed at the same location in the two standard and PCM walls as well as the rooms and then used to read the temperature of the south wall outer surface and inner surface in addition to the PCM and room temperature for both standard and test rooms (room-A and room-B).

#### II. Weather Station

The weather station consists basically of three sensors as shown in Figure 12. The first sensor is a 108-probe used to measure the ambient air temperature. The second sensor is the three-cup NRG#40 anemometers developed by the NRG system were used to measure the wind speed. The last sensor is the CS300 pyranometer provided by Campbell Scientific which is used to measure the total solar radiation.



Figure 12: Weather Station

#### III. Pyranometer

The solar intensity on the south wall was measured using a small pyranometer model TES-1333/1333R calibrated with an accuracy of  $\pm 5\%$ .

## 4. EXPERIMENTAL PROCEDURE

### I. Design of the Model

The model was designed by SOLIDWORKS software as shown in Figure 1, top views figures and the schematic figures mentioned before, then fabricated as shown in Figure 2.

### II. Set Up the Measurement Tools

The weather station is established close to the model while the temperature sensors are fixed in the same location at both the standard room as shown in Figure 4 and the test rooms are shown in Figure 8 and Figure 11. to measure the temperature every 15 minutes. Both the weather station sensors and temperature sensors are connected to data loggers connect to a computer placed in the control room to record the data measured.

### III. Test procedure

According to the temperature diagram, Figure 13 demonstrates the ambient temperature variations in the Al-Diwaniya city in 2019. These values predicted by Meteonorm software, the figure shows that the peak temperature period between week 24 and week 35 of the year, where this period is the hottest in Iraq lies in July and August so that the first test (test model-A) was done on the 17 of August and the second test (test model-B) was done on the 18 of August. However, these days were picked out to test the PCM performance in the highest weather temperature period. In this study, two outdoor tests were made for two rooms with and without PCM a long 24 hours in the Al-Diwaniya city (latitude: 32.14° and longitude: 44.94°) in Iraq. The test included recording the temperatures, wind speed, and solar radiation.

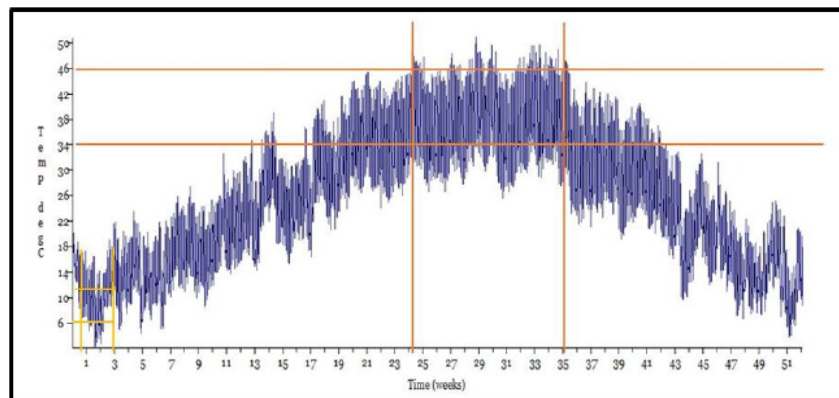


Figure 13: Predicted Temperature Profile of 2019 in Diwaniyah City

## 5. RESULTS AND DISCUSSION

### I. Results of Test Model A

Figure 14 demonstrates the variation of temperature of the external layer of the south wall of the two rooms with and without PCM. From this figure, it is shown that the temperature on the wall with PCM (TW-A) is slightly less than that on the wall without PCM (NTW) due to the cooling effect of PCM during charging time while at discharging time the temperature on the outer surface of TW-A will be more than that of NTW due to the heat released from the PCM to the surrounding during discharging time. Figure 15 demonstrates the temperature profile on both the inner surface of the south wall with and without PCM. The temperature on the inner surface of the wall with PCM (TW-A) is less than that on the corresponding location on the wall without PCM (NTW) with 2.7 °C due to the insulation role of PCM where PCM absorb a large amount of heat during phase change so that it will increase the thermal insulation inside the wall. Also, from this figure, it can be concluded that the PCM increases the time lag by 1 hour and that will shift the peak load where:

$$\tau_l = \tau_{TW,peak} - \tau_{NTW,peak} \quad (1)$$

Figure 16 showed that the temperature variation of both the standard and test rooms. The peak reduction in the temperature of the test room-A was 2.7 °C compared with the standard room due to the insulating effect of PCM that was used in TW-A. [10]

## II. Results of Test Model B

Figure 17 showed the temperature profiles of the external layer of the south wall of the two rooms with and without PCM. From this figure, it is shown that the temperature on the TW-B is slightly less than that on the NTW due to the cooling effect of PCM during charging time while at discharging time the temperature on the outer surface of TW-B will be more than that of NTW due to the heat released from the PCM to the surrounding during the discharging time. Figure 18 illustrated the temperature variations on both the inner surface of the south wall with and without PCM of model-B. The temperature on the inner surface of the wall with PCM (TW-B) is less than that on the corresponding location on the wall without PCM (NTW) with 1.9 °C due to the insulation role of PCM where PCM absorb a large amount of heat during phase change so that it will increase the thermal insulation inside the wall. Also, from this figure and by using Eq. (1), it can be concluded that the PCM increases the time lag by 1 hour and that will shift the peak load by 1 hour. Figure 19 demonstrated the temperature profiles of both the standard and test rooms for model B. The peak reduction in the temperature of the test room-B was 1.9 °C compared with the standard room due to the insulating effect of PCM that was used in TW-B.

## III. Uncertainty Analysis

To evaluate the measurement uncertainties, an error analysis of the experimental data was performed. It is possible to obtain total uncertainty by combining the accuracy of the sensor and the accuracy of the measuring instrument in each measurement. By taking the square root of the sum of the individual errors, the root sum of squares method is the most realistic method. [16]–[18].

$$\delta_{total} = \sqrt{(\delta_{sensor})^2 + (\delta_{instrument})^2} \quad (2)$$

$$Min. \& Max. Uncer. (\%) = \left( \frac{\delta_{total}}{Min. \& Max. Reading} \right) \times 100 \quad (3)$$

Where  $\delta_{total}$  is total uncertainty,  $\delta_{sensor}$  is sensor uncertainty and  $\delta_{instrument}$  is measuring device uncertainty. Furthermore, in this study, the appropriate measuring device accuracy is shown in Table II. The main parameters measured by these devices were: temperature, solar radiation, and velocity of the wind. Table III showed the uncertainties and error percentages.

TABLE II: Measurement device's accuracy

Measurement devices	Accuracy
K-type thermocouple	±4% °C
Applent data logger	±4% °C
Solar power meter	±5% W/m <sup>2</sup>
Anemometer	± (2%+0.2 m/sec)

TABLE III: Uncertainties and Errors Percentages

Parameters	Uncertainty	Error %
Indoor temperature difference	±0.566	5.01
Solar irradiation	±5	1.13
Wind speed	±0.26	8.667

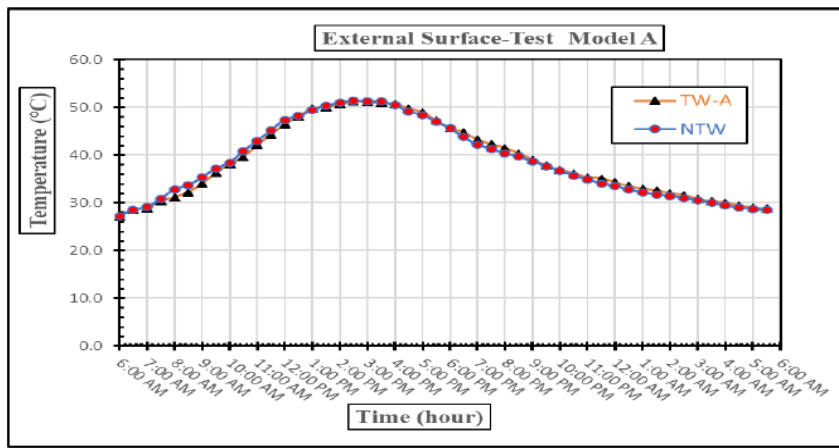


Figure 14: External Surface Temperature of TW-A and NTW

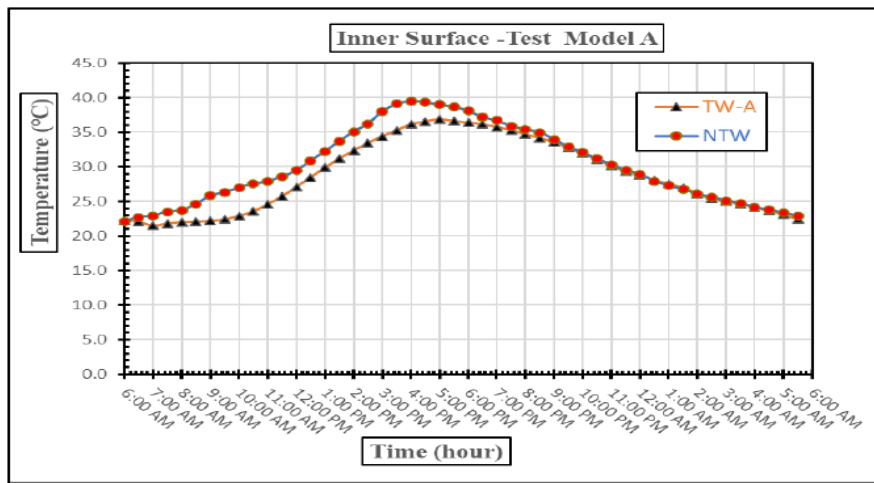


Figure 15: Inner Surface Temperature of TW-A and TW

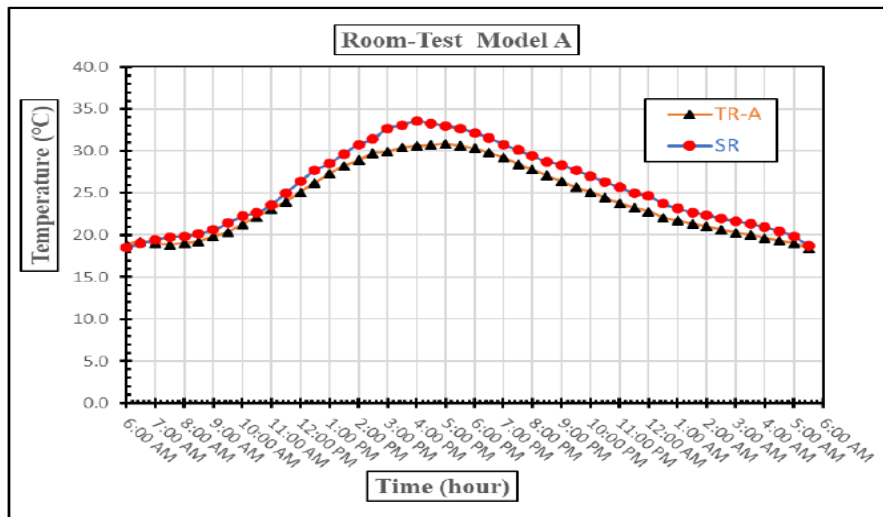


Figure 16: Temperature of Test Room-A and Standard Room

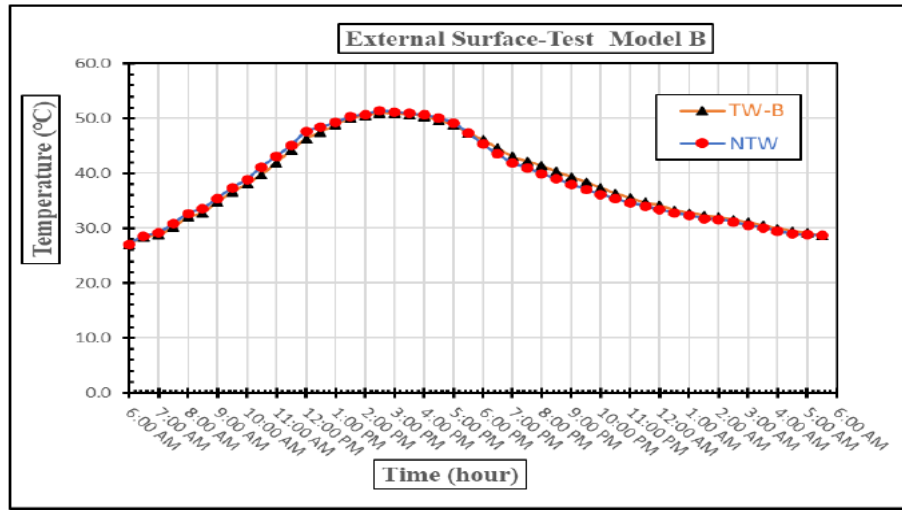


Figure 17: Temperature of External Surface of TW-B and NTW

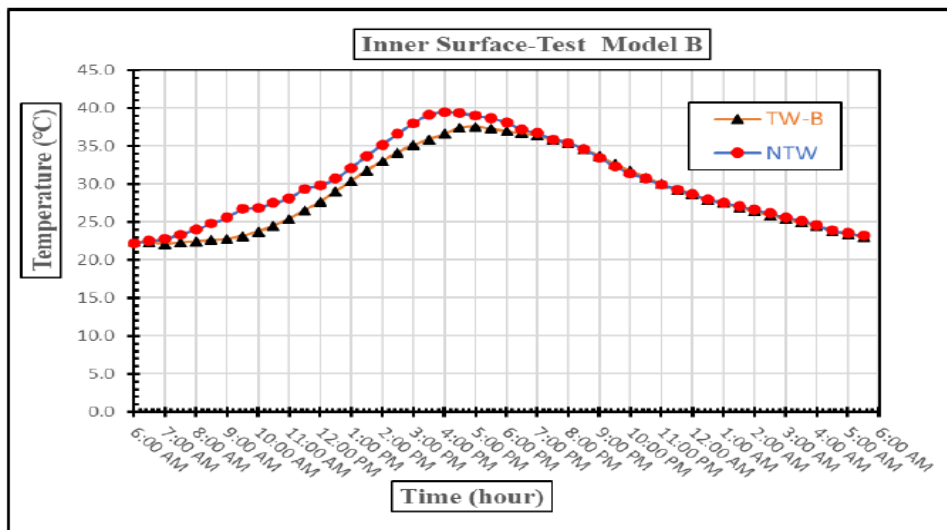


Figure 18: Temperature of Inner Surface of TW-B and NTW

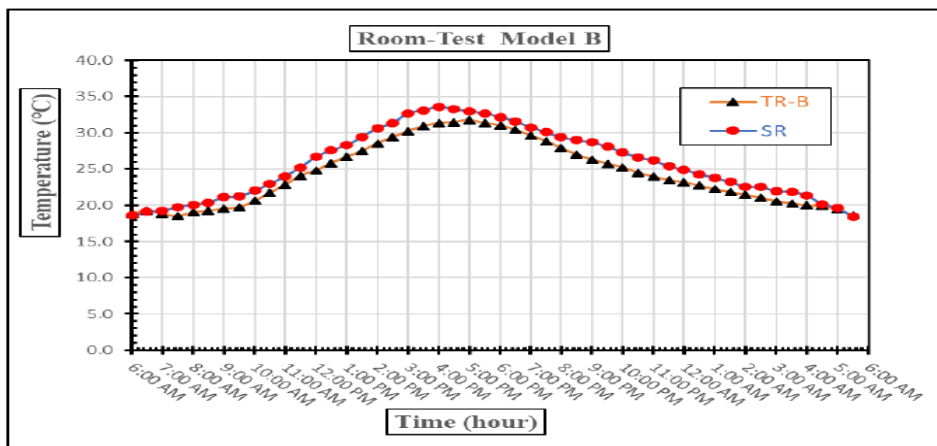


Figure 19: Temperature of Test Room-A and Standard Room

## 6. CONCLUSIONS

The utilization of PCM as thermal insulation materials had been investigated experimentally in two models. Test model-A where the PCM capsules inserted in the inner rows of hollow bricks that forming the TW-A while, in test model-B, the PCM capsules were inserted into the outer rows of the hollow bricks that forming TW-B. From the obtained results we conclude the following points:

- 1) Reduction in the inner surface of the TW-A by about 2.7°C compared to the wall without PCM (NTW).
- 2) Reduction in the test room-A air temperature by 2.7°C compared to the standard room.
- 3) Reduction in the inner surface of the TW-B by about 1.9 °C compared to the wall without PCM (NTW).
- 4) Reduction in the test room-B air temperature of 1.9 °C compared to the standard room.
- 5) From the reduction in the inner temperature of the PCM wall (TW-A or TW-B), it can be concluded that the use of PCM will lead to an increase in the stored heat in TW more than that stored in NTW and that will cause a reduction in the heat gain entering the room.
- 6) For the two models, the time lag increased by 1 hour and that shifted the peak load to 1 hour.
- 7) From the obtained results, it can be concluded that the test model-A is better than the test model-B and the optimum location of PCM capsules is at the inner rows of the hollow bricks because it offers the best thermal performance for the test wall and test room.

### Nomenclature:

$\tau_l$ : Time lag (hour)

$\tau_{TW,peak}$ : Time corresponds to peak temperature on TW (hour)

$\tau_{NTW,peak}$ : Time corresponds to peak temperature on NTW (hour)

$\tau_{NTW,peak}$ : Time corresponds to peak temperature on NTW (hour)

### Abbreviation:

PCM: Phase change material

TW: Wall with PCM capsules (treated wall or test wall)

TW-A: Wall with PCM capsules at the inner rows of the cavities of hollow bricks

TW-B: Wall with PCM capsules at the outer rows of the cavities of hollow bricks

NWT: Wall without PCM capsules (untreated wall or domestic wall)

TR-A: Test room with TW-A

TR-B: Test room with TW-B

SR: Standard room (room without PCM wall)

## REFERENCES

- [1] M. I. Hasan, H. O. Basher, A. O. Shdhan, Experimental investigation of phase change materials for insulation of residential buildings, *Sustain. Cities. Soc.*, 36 (2018) 42–58. <http://dx.doi.org/10.1016/j.scs.2017.10.009>
- [2] E. M. Alawadhi, Thermal analysis of a building brick containing phase change material, *Energy Build.*, 40 (2008) 351–357. <http://dx.doi.org/10.1016/j.enbuild.2007.03.001>
- [3] A. Castell, I. Martorell, M. Medrano, G. Pérez, L. F. Cabeza, Experimental study of using PCM in brick constructive solutions for passive cooling, *Energy. Build.*, 42 (2010) 534– 540. <http://dx.doi.org/10.1016/j.enbuild.2009.10.022>
- [4] Y. Quanying, H. Ran, L. Lisha, Experimental study on the thermal properties of the phase change material wall formed by different methods, *Sol. Energy.*, 86 (2012) 3099–3102. <http://dx.doi.org/10.1016/j.solener.2012.07.022>
- [5] X. Kong, S. Lu, J. Huang, Z. Cai, S. Wei, Experimental research on the use of phase change materials in perforated brick rooms for cooling storage, *Energy. Build.*, 62 (2013) 597–604. <http://dx.doi.org/10.1016/j.enbuild.2013.03.048>
- [6] X. Jin, M. A. Medina, X. Zhang, On the importance of the location of PCMs in building walls for enhanced thermal performance, *Appl. Energy.*, 106 (2013) 72–78. <http://dx.doi.org/10.1016/j.apenergy.2012.12.079>

- [7] S. D. Zwanzig, Y. Lian, E. G. Brehob, Numerical simulation of phase change material composite wallboard in a multi-layered building envelope, ASME Int. Mech. Eng. Congr. Expo. Proc., 6 (2013) 1143–1157. <http://dx.doi.org/10.1115/IMECE2012-89526>
- [8] K. O. Lee, M. A. Medina, X. Sun, On the use of plug-and-play walls (PPW) for evaluating thermal enhancement technologies for building enclosures: Evaluation of a thin phase change material (PCM) layer, Energy. Build., 86 (2015) 86–92. <http://dx.doi.org/10.1016/j.enbuild.2014.10.020>
- [9] F. Guarino, V. Dermardiros, Y. Chen, J. Rao, A. Athienitis, M. Cellura, M. Mistretta, PCM thermal energy storage in buildings: Experimental study and applications, Energy. Procedia., 70 (2015) 219–228. <http://dx.doi.org/10.1016/j.egypro.2015.02.118>
- [10] A. Hasan, K. A. Al-Sallal, H. Alnoman, Y. Rashid, S. Abdelbaqi, Effect of phase change materials (PCMs) integrated into a concrete block on heat gain prevention in a hot climate, Sustain., 8 (2016) 1009. <http://dx.doi.org/10.3390/su8101009>
- [11] X. Jin, M. A. Medina, X. Zhang, Numerical analysis for the optimal location of a thin PCM layer in frame walls, Appl. Therm. Eng., 103 (2016) 1057–1063. <http://dx.doi.org/10.1016/j.applthermaleng.2016.04.056>
- [12] A. Fateh, D. Borelli, F. Devia, H. Weinläeder, Dynamic modelling of the solar radiation exposure effects on the thermal performance of a PCMs-integrated wall, Int. J. Heat. Technol., 35 (2017) S123–S129. <http://dx.doi.org/10.18280/ijht.35Sp0117>
- [13] M. Ning, H. Jingyu, P. Dongmei, L. Shengchun, S. Mengjie, Investigations on thermal environment in residential buildings with PCM embedded in external wall, Energy. Procedia., 142 (2017) 1888–1895. <http://dx.doi.org/10.1016/j.egypro.2017.12.387>
- [14] O. R. Labed, M. B. Al-hadithi, O. T. Fadhil, Experimental Investigation of Heat Reduction through Walls Using Phase Change Material, Anbarj. Eng. Sci., 7 (2018) 245–251. <http://dx.doi.org/10.37649/AENGS.2018.145976>
- [15] S. Kumar, S. A. Prakash, R. Velraj, Effect of phase change material integration in clay hollow brick composite in building envelope for thermal management of energy efficient buildings, J. Build. Phys., 43 (2019). <https://doi.org/10.1177/1744259119867462>
- [16] J. P. Holman, Experimental Methods for Engineers, Mcgraw-hill Ser. Mec. Engi., (2012).
- [17] P. R. Bevington, D. K. Robinson, Data reduction and error analysis, phys. sci., (2003).
- [18] H. A. A. Wahhab, A. R. A. Aziz, H. H. Al-Kayiem, M. S. Nasif, L. O. Afolabi, Prediction of the phase distribution of diesel/CNG bubbly flow in a horizontal pipe under the influence of a magnetic field, J. Mech. Sci. Technol., 31 (2017) 5299–5309. <https://doi.org/10.1007/s12206-017-1024-1>